Int. J. Multiphase Flow Vol. 14, No. 2, pp. 175–187, 1988
Printed in Great Britain.

0301-9322/88 $3.00 + 0.00

THE INFLUENCE OF NON-CONDENSIBLE GAS ON TWO-PHASE CRITICAL FLOW

G. P. CELATA, M. CUMO, F. D'ANNIBALE and G. E. FARELLO
ENEA Casaccia TERM/ISP Heat Transfer Laboratory, Via Anguillarese 301, 00060 Rome, Italy

(*Received* 7 *April* 1987; *in revised form* 25 *October* 1987)

Abstract—The present paper deals with a two-phase steam–water critical flow experiment in long tubes, in which known air flow rates are injected into the stagnation region. The aim of the experiment is to detect the influence of non-condensible gas on the two-phase critical mass flux as well as to establish the limit, in terms of air concentration, beyond which the critical flow is affected by the presence of the gas. The test section is a vertical, circular channel with i.d. 4.6 mm and a length of 1500 mm ($L/D = 325$). Results of experiments with initially subcooled liquid (together with some data from saturated liquid discharges), up to pressures of 1.5 MPa are reported together with the analysis of the effects of the non-condensibles under the different stagnation conditions.

1. INTRODUCTION

In nuclear reactor safety analyses, the most serious accident sequences are represented by those caused by a break in the pressure boundary of the primary loop.

During the last few years, both experimental and theoretical studies concerning this kind of accident have been intensified because of the growing attention paid to the so-called "small break" LOCAs (SB-LOCA), especially after the 1979 Three Mile Island accident.

An SB-LOCA, in comparison to a "large break" LOCA (LB-LOCA), has, among others, two main disadvantages which make it more important for consideration:

(a) an SB-LOCA has a potential occurrence frequency much higher than that of an LB-LOCA because of the larger number of small diameter pipes;
(b) since human actions to mitigate the consequences of the accident are possible, an in-depth knowledge of the transient following the break is required.

Research in the broad area devoted to the analysis of the above-mentioned problems has been reported by Ardron (1978), Dobran (1985), Flinta (1983), Henry (1968, 1970a, b), Henry & Fauske (1971), Ilic *et al.* (1986), Lackmé (1982), Moody (1965, 1966), Reocreux (1974, 1976), Weigand *et al.* (1983) and in various *Proceedings* (1981, 1983, 1985) as far as the international situation is concerned. ENEA theoretical and experimental contributions on two-phase steam–water critical flows have been reported by Celata *et al.* (1983a, b, 1985, 1986a, b).

Very little information is available in the literature about the influence of non-condensible gas on the critical two-phase flow behaviour with respect to a reference situation (degassed liquids). On the other hand, in a nuclear reactor, under severe accident conditions, the rate at which non-condensibles can be released into the coolant is significant.

The situation is also of great interest for safety considerations in the chemical industry.

In the present work, an experiment on critical two-phase flows with air injected into the two-phase steam–water mixture is reported and the results are discussed.

2. THE EXPERIMENTAL SETUP

The experimental tests were carried out with the steam–water loop sketched in figure 1. The loop consists of two cylindrical pressure vessels, each having a capacity of 100 l., an electric heater (10 kW) for water heating and a centrifugal pump for the recirculation of the liquid from the main vessel (S_1) through the electric heater.

Vessel S_1, filled with demineralized water, simulates the reference pressure vessel, whilst vessel S_2 allows volumetric expansion of the water during heating and acts as a pressurizer: it is partially filled with cold water and pressurized with nitrogen.

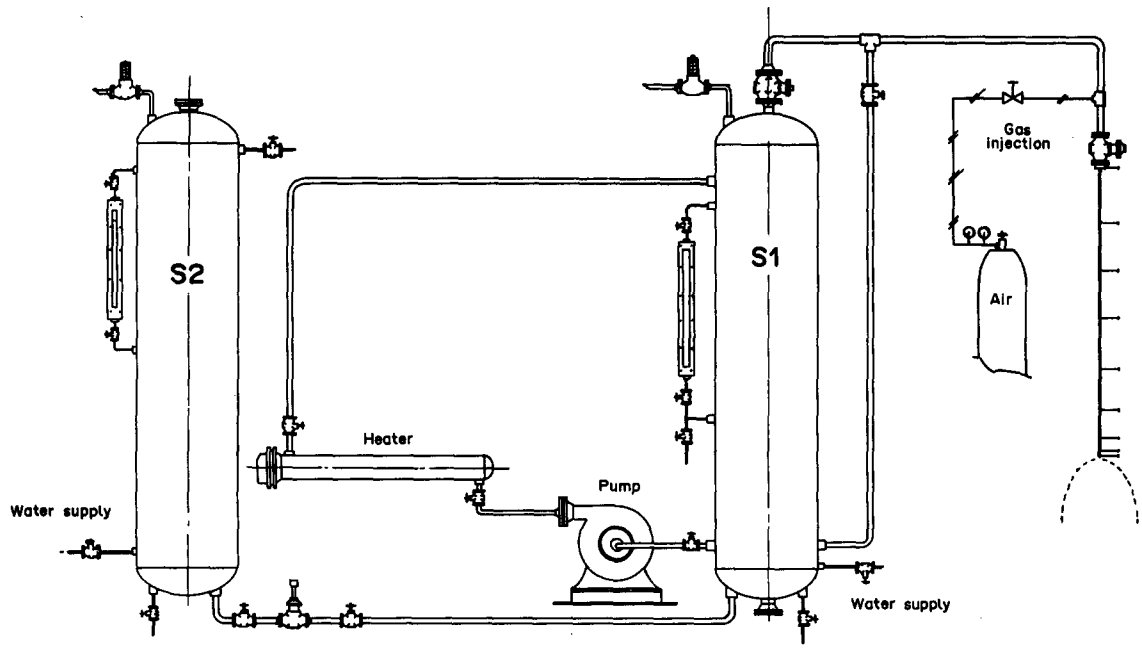

Figure 1. Schematic of the experimental setup.

Referring to the tests with initially subcooled liquid, water flows out from the upper plenum of vessel S_1, and with a quick-opening valve is discharged through the test channel. During the subcooled tests, vessel S_1 is always full of liquid because of the liquid flow coming from vessel S_2; consequently, the discharged mass flow rate can be measured, with the necessary density correction, by means of a turbine flowmeter placed on the connection leg between S_1 and S_2.

The cold water ($\sim 60°C$) from S_2 is introduced into vessel S_1 from the bottom: so, considering the average time of the test (~ 20 s), the maximum mass flow rate during the discharge ($\leqslant 0.2$ kg/s) and the capacity of the vessel (100 l.), the water at the exit of the upper plenum of S_1 is maintained at constant thermodynamic conditions.

For the tests with initially saturated liquid, water flows out from the lower plenum of vessel S_1 that is disconnected from S_2. In this case, the mass flow rate measurement is obtained by collecting the outflowing mixture in a tank filled with ice, and weighing the discharged fluid over the measured test time. The technique gives generally good results because of the quasi-steady-state stagnation conditions during the tests.

Air, which represents the non-condensible gas phase, is injected through a calibrated nozzle just upstream of the test section. Air flow rate is measured by means of sonic calibrated disks (air pressure and temperature are measured upstream of the disks). The test section, already employed in previous experiments (Celata *et al.* 1983a, 1986b), consists of a straight vertical channel, a round duct instrumented with six thermocouples and six pressure taps; i.d. = 4.6 mm, length = 325 dia. The inlet is of the rounded-edge type.

3. TEST MATRIX AND EXPERIMENTAL RESULTS

The influence of known amounts of non-condensible gas on the critical two-phase flow was studied by carrying out 132 tests with initially subcooled and saturated water discharges, in addition to the reference tests without non-condensible gas.

The range of variation in the parameters in the experiments are as follows:

stagnation pressure, p_0	0.5, 1.0 and 1.5 MPa
inlet subcooling, ΔT_{sub}	0, 20, 40 and 60°C.

The air mass flow rate ranges between the minimum value detectable with the available instrumentation ($>2 \cdot 10^{-2}$ g/s) and the maximum one which allows an acceptable stability of the flow (<1.5 g/s).

The experimental results of the 132 tests are summarized in table 1, where the following variables are reported for each run:

stagnation pressure, p_0;
stagnation temperature, T_0;
inlet subcooling, ΔT_{sub};
outlet critical pressure, p_c;
reference critical mass flux without non-condensible gas, G_{c0};
critical mass flux with non-condensible gas, G_c;
air mass flux, G_a;

and

ratio between G_c and G_{c0}, R.

The G_{c0} values, reported in table 1, are measured at the same stagnation conditions, p_0 and T_0, as the G_c measurements.

The outlet pressure is measured near the exit of the tube; the distance between the exit and the last pressure tap is 5 mm.

The mass fluxes are computed by dividing the flow rates by the cross section of the test channel.

In tables 2 and 3 pressures and temperatures measured along the test channel are reported for some tests. In figure 2 typical pressure profiles along the discharge channel are plotted for subcooled and saturated tests. This information could be useful in the assessment of detailed mechanistic models.

4. DATA ANALYSIS

The experimental results are plotted in figure 3, except those of the saturated liquid tests, which will be discussed later. The ratio, R, between the actual specific mass flow rate, G_c, and the reference one, G_{c0}, is plotted vs the ratio Q_a/Q_{c0}; Q_a represents the air volumetric flow rate, whilst Q_{c0} represents the reference critical volumetric flow rate, both computed at stagnation conditions.

From data analysis, in fact, it appears that Q_a/Q_{c0} is the most significant parameter in describing the behaviour of R. The presence of non-condensible gas reduces the cross section available for the steam–water flow, giving rise to a flow resistance which is obviously linked to the specific volume of the air.

Considering figure 3, some comments may be derived. Tests with the same inlet subcooling show a similar trend, not dependent on either stagnation pressure or stagnation temperature. The trend of the ratio R vs Q_a/Q_{c0} seems to depend only on inlet subcooling, at least within the ranges of stagnation conditions investigated.

Regarding the influence of non-condensible gas on the two-phase critical mass flux, no threshold or limit was observed, in the sense that even a very small quantity of air produces a reduction in the mass flux.

As far as the saturated liquid tests are concerned, the experimental data show a wide and random spread around the average trend of the subcooled data. Unfortunately, these tests have revealed a strong fluid-dynamic instability of the flow, decreasing the reproducibility of the data and increasing the errors associated with the measurements. It is probable that the injection of even a small quantity in weight of cold air into a liquid at saturation conditions, (incidentally, also in the presence of local agglomerates of bubbles on the metallic walls), produces a de-stabilizing effect on the flow, spoiling the experimental measurements.

Data analysis has been accomplished using two different approaches: an empirical approach and a theoretical one based on previous work by the authors (Celata *et al.* 1983a).

The empirical approach

The parameter R defined above has been correlated to the amount of non-condensible gas injected and to the stagnation conditions. As discussed above, the injected air is represented by the ratio between the volumetric flow rate of air, Q_a, and the volumetric reference critical flow rate without air, Q_{c0}.

Table 1

	p_0 (MPa)	T_0 (°C)	ΔT_{sub} (°C)	p_c (MPa)	G_{c0}	G_c (kg/m^2 s)	G_a	$\frac{G_c}{G_{c0}}$
77	1.012	120.45	59.95	0.207	10,041	9178	2.22	0.914
78	1.009	120.21	60.06	0.210	10,047	8795	3.36	0.875
79	1.057	120.21	62.10	0.222	10,203	8322	7.49	0.815
80	1.039	120.70	60.85	0.217	10,035	9250	5.03	0.922
81	1.036	120.70	60.72	0.225	10,035	8154	10.84	0.813
82	1.038	120.21	61.30	0.225	10,047	8010	13.66	0.797
84	1.001	120.70	59.23	0.213	10,035	6740	18.45	0.672
85	1.079	120.94	62.27	0.218	10,185	6584	27.80	0.646
86	1.081	120.70	62.59	0.202	10,035	5799	43.56	0.578
87	1.067	120.70	62.02	0.206	10,191	6273	35.11	0.615
88	1.068	120.45	62.31	0.192	10,041	5254	54.94	0.523
89	1.067	120.70	62.02	0.186	10,035	4703	67.52	0.469
90	1.065	120.94	61.69	0.182	10,029	4230	79.20	0.422
119	1.563	138.62	61.62	0.330	11,509	6578	79.92	0.571
120	1.483	138.38	59.36	0.345	11,515	7028	51.82	0.610
121	1.468	138.38	58.88	0.367	11,515	8076	27.74	0.701
122	1.430	138.62	57.40	0.362	11,509	8519	22.11	0.740
123	1.467	138.62	58.61	0.362	11,509	9268	15.88	0.805
124	1.437	138.62	57.63	0.356	11,509	9718	7.43	0.844
125	1.428	138.62	57.34	0.344	11,509	10,161	3.36	0.883
50	0.516	112.11	40.93	0.139	6728	5128	2.70	0.762
51	0.513	112.11	40.71	0.139	6728	5284	2.22	0.786
52	0.511	111.87	40.80	0.140	6734	5452	1.68	0.809
53	0.509	112.11	40.41	0.141	6728	5847	1.14	0.869
54	0.517	111.87	41.24	0.132	6734	4487	5.93	0.667
55	0.513	112.11	40.71	0.135	6728	4643	4.85	0.691
56	0.512	112.11	40.63	0.135	6728	4805	3.95	0.714
57	0.529	112.60	41.38	0.152	6722	5116	3.36	0.762
58	0.529	112.60	41.38	0.140	6722	3840	11.98	0.571
59	0.515	111.87	41.10	0.139	6734	4170	8.69	0.619
60	0.518	112.11	41.07	0.141	6728	4487	7.01	0.667
61	0.544	112.36	42.69	0.127	6722	3199	15.04	0.476
62	0.539	112.11	42.59	0.120	6728	2402	23.49	0.357
63	0.544	112.36	42.69	0.123	6722	2960	18.69	0.440
65	0.545	112.11	43.01	0.118	6728	2241	30.02	0.333
20	0.975	143.05	35.73	0.355	8118	8118	0.00	1.000
21	1.002	141.08	38.88	0.298	8310	5194	18.63	0.625
22	0.993	141.57	38.00	0.287	8447	4889	22.29	0.579
24	1.051	140.59	41.46	0.272	8621	4457	34.87	0.517
25	1.039	140.35	41.20	0.261	8627	4014	42.48	0.465
27	1.056	140.10	42.16	0.251	8633	4020	50.80	0.465
28	1.045	140.35	41.46	0.281	8627	4907	26.96	0.569
29	1.061	140.35	42.12	0.285	8627	5057	26.90	0.586
30	1.046	139.36	42.48	0.222	8651	2984	76.27	0.345
31	1.069	139.36	43.44	0.234	8651	3583	66.74	0.414
32	1.058	139.61	42.74	0.243	8645	3876	54.52	0.448
33	1.009	139.85	40.42	0.327	8639	6704	7.31	0.776
34	1.008	140.10	40.13	0.331	8633	6998	5.93	0.810
35	1.005	140.10	40.00	0.332	8633	7141	4.79	0.828
36	1.003	139.61	40.40	0.307	8645	5961	15.76	0.690
37	0.998	139.61	40.18	0.316	8645	6261	13.00	0.724
38	0.997	139.85	39.90	0.320	8639	6554	10.66	0.759
39	1.048	140.10	41.83	0.300	8633	5805	21.75	0.672
40	1.017	139.61	41.01	0.304	8645	5961	17.91	0.690
41	1.014	139.85	40.63	0.311	8639	6105	14.92	0.707
42	1.027	139.61	41.43	0.328	8645	7525	3.30	0.871
43	1.013	139.85	40.59	0.333	8789	7597	2.76	0.864
44	1.011	140.10	40.26	0.334	8633	7741	2.22	0.897
112	1.416	158.06	37.50	0.487	9580	6620	22.59	0.691
113	1.492	158.31	39.72	0.537	9712	8729	3.36	0.899
114	1.465	158.06	39.10	0.529	9724	8028	7.49	0.826
115	1.504	157.08	41.33	0.517	9754	7776	16.18	0.797
116	1.515	158.31	40.45	0.484	9784	6614	27.50	0.676
117	1.569	158.06	42.36	0.443	9724	5919	51.04	0.609
118	1.565	157.32	42.98	0.392	9885	4943	78.06	0.500
67	0.509	131.74	20.78	0.214	5027	3427	2.76	0.682
68	0.506	131.74	20.56	0.217	5027	3505	2.28	0.697
69	0.543	132.24	22.75	0.233	5021	4182	1.68	0.833

—continued

Table 1—*continued*

	p_0 (MPa)	T_0 (°C)	ΔT_{sub} (°C)	p_c (MPa)	G_{c0}	G_c (kg/m² s)	G_a	$\frac{G_c}{G_{c0}}$
70	0.536	131.50	22.99	0.234	5033	4421	1.14	0.879
72	0.529	131.74	22.24	0.197	5182	3199	5.03	0.618
73	0.520	131.50	21.83	0.203	5033	3355	3.71	0.667
74	0.516	131.25	21.79	0.160	5033	1833	13.90	0.364
75	0.512	131.25	21.49	0.183	5188	2594	8.09	0.500
76	0.520	131.99	21.34	0.170	5027	2133	10.78	0.424
91	1.055	159.30	22.92	0.492	6878	5542	3.36	0.806
92	1.040	159.54	22.05	0.508	6872	5751	2.22	0.837
93	1.036	159.54	21.88	0.488	6872	5188	4.97	0.755
94	1.039	159.30	22.25	0.462	6878	4913	6.35	0.714
95	1.045	159.54	22.26	0.442	6872	4769	7.49	0.694
96	1.048	159.79	22.14	0.389	6866	4206	16.00	0.612
97	1.043	159.79	21.93	0.414	6866	4344	13.48	0.633
98	1.053	159.79	22.35	0.440	6866	4901	10.72	0.714
99	1.060	159.54	22.88	0.351	7010	3643	21.57	0.520
100	1.061	159.54	22.93	0.324	7010	3223	27.92	0.460
101	1.060	159.30	23.13	0.281	7016	2384	52.18	0.340
102	1.123	159.79	25.19	0.319	7147	2942	44.69	0.412
103	1.110	160.03	24.43	0.332	7141	3217	36.07	0.451
104	1.098	152.15	31.83	0.401	7321	2438	69.44	0.333
105	1.507	176.56	21.95	0.396	7393	2774	81.84	0.375
106	1.479	176.56	21.06	0.429	7393	3301	52.54	0.446
107	1.461	175.32	21.72	0.414	7429	3451	27.14	0.464
108	1.460	177.54	19.46	0.545	7363	4601	22.71	0.625
109	1.467	177.30	19.93	0.605	7375	5003	16.30	0.679
110	1.476	177.54	19.98	0.676	7363	5524	7.37	0.750
111	1.441	177.79	18.60	0.751	7357	5913	3.30	0.804
143	1.090	168.17	15.49	0.582	5853	4224	2.88	0.721
144	1.091	168.17	15.50	0.599	5991	4901	2.22	0.818
139	1.028	174.33	6.75	0.453	3864	3061	18.63	0.793
140	1.032	174.09	7.16	0.317	3864	2265	22.65	0.586
141	1.063	174.09	8.46	0.299	3732	2001	27.38	0.536
142	1.022	173.59	7.23	0.314	3738	1534	18.63	0.411
126	0.490	147.72	3.37	0.283	11,042	11,042	0.00	1.000
127	0.486	148.22	2.57	0.166	10,425	6824	2.88	0.619
128	0.491	149.94	1.23	0.160	10,365	6506	1.86	0.593
129	0.492	149.20	2.04	0.183	10,269	6956	1.14	0.640
130	0.494	149.45	1.95	0.161	10,383	6369	5.75	0.580
131	0.524	150.68	2.95	0.172	10,215	7357	3.77	0.680
132	0.511	150.43	2.24	0.162	10,227	6926	8.15	0.640
133	0.481	149.20	1.20	0.145	10,269	6890	10.78	0.634
134	0.481	144.28	6.12	0.139	10,431	6896	14.92	0.626
135	0.474	149.45	0.40	0.119	10,257	5793	23.19	0.533
136	0.477	148.22	1.87	0.128	10,299	5847	18.57	0.536
161	0.478	148.95	1.21	0.154	10,185	6656	2.82	0.654
163	0.482	148.46	2.01	0.175	10,203	7974	1.14	0.782
164	0.465	147.97	1.17	0.149	10,215	6866	3.71	0.672
162	0.481	147.97	2.43	0.166	10,215	7249	1.92	0.710
165	0.467	148.22	1.08	0.137	10,209	6902	5.75	0.676
166	0.461	146.00	2.82	0.133	10,281	5722	15.22	0.557
167	0.466	147.48	1.74	0.143	10,233	6369	10.90	0.623
137	0.962	177.79	0.41	0.408	11,665	11,665	0.00	1.000
138	0.968	177.05	1.42	0.299	11,701	7908	3.36	0.676
145	0.945	176.80	0.63	0.287	11,713	8148	3.41	0.696
146	0.978	176.56	2.36	0.340	11,725	8705	7.49	0.743
147	0.945	177.05	0.39	0.286	11,701	7447	5.03	0.637
148	0.923	174.33	2.09	0.274	11,820	9053	10.72	0.766
149	0.920	174.83	1.46	0.229	11,803	9166	17.01	0.777
150	0.955	177.05	0.84	0.247	11,701	7501	27.26	0.641
151	0.948	176.56	1.02	0.229	11,725	8250	22.95	0.704
152	0.947	175.08	2.45	0.269	11,791	9376	18.75	0.796
153	0.956	176.80	1.13	0.256	11,713	7651	35.65	0.654
154	0.955	177.79	0.10	0.418	12,012	12,012	0.00	1.000
156	1.448	193.35	3.26	0.350	12,414	10,574	27.56	0.852
157	1.422	194.59	1.18	0.595	12,330	10,173	23.78	0.825
158	1.429	195.08	0.91	0.588	12,294	10,317	16.30	0.839
159	1.430	195.58	0.45	0.449	12,258	9909	7.67	0.809
160	1.411	194.34	1.06	0.464	12,348	11,509	3.41	0.932

Table 2

	Pressures (MPa)					
	p_0	p_1	p_2	p_3	p_4	p_5
20	0.975	0.896	0.772	0.512	0.394	0.355
21	1.002	0.944	0.847	0.604	0.415	0.298
22	0.993	0.944	0.859	0.609	0.399	0.287
24	1.051	0.996	0.888	0.620	0.407	0.272
25	1.039	0.992	0.897	0.614	0.383	0.261
27	1.056	1.010	0.920	0.622	0.377	0.251
28	1.045	0.997	0.883	0.623	0.414	0.281
29	1.061	1.006	0.904	0.629	0.416	0.285
30	1.046	1.013	0.927	0.586	0.354	0.222
31	1.069	1.032	0.915	0.618	0.378	0.234
32	1.058	1.018	0.916	0.627	0.370	0.243
33	1.009	0.950	0.839	0.599	0.438	0.327
34	1.008	0.943	0.829	0.588	0.434	0.331
35	1.005	0.939	0.822	0.579	0.430	0.332
36	1.003	0.950	0.839	0.603	0.425	0.307
37	0.998	0.947	0.835	0.604	0.436	0.316
38	0.997	0.942	0.830	0.598	0.434	0.320
39	1.048	0.995	0.882	0.632	0.424	0.300
40	1.017	0.968	0.858	0.613	0.423	0.304
41	1.014	0.960	0.849	0.613	0.428	0.311
42	1.027	0.959	0.835	0.578	0.422	0.328
43	1.013	0.945	0.819	0.568	0.422	0.333
44	1.011	0.938	0.821	0.563	0.414	0.334
126	0.490	0.481	0.460	0.438	0.371	0.283
127	0.486	0.475	0.443	0.346	0.241	0.166
128	0.491	0.487	0.448	0.368	0.242	0.160
129	0.492	0.488	0.463	0.390	0.279	0.183
130	0.494	0.489	0.467	0.367	0.243	0.161
131	0.524	0.519	0.500	0.398	0.260	0.172
132	0.511	0.508	0.485	0.387	0.251	0.162
133	0.481	0.478	0.450	0.343	0.213	0.145
134	0.481	0.476	0.441	0.328	0.206	0.139
135	0.474	0.465	0.424	0.313	0.182	0.119
136	0.477	0.476	0.437	0.327	0.201	0.128
154	0.955	0.944	0.918	0.838	0.605	0.418
137	0.962	0.952	0.927	0.829	0.591	0.408
138	0.968	0.957	0.902	0.712	0.460	0.299
145	0.945	0.936	0.882	0.696	0.450	0.287
146	0.978	0.973	0.937	0.817	0.533	0.340
147	0.945	0.936	0.873	0.690	0.453	0.286
148	0.923	0.904	0.826	0.629	0.418	0.274
149	0.920	0.908	0.859	0.655	0.381	0.229
150	0.955	0.943	0.856	0.645	0.401	0.247
151	0.948	0.929	0.877	0.630	0.363	0.229
152	0.947	0.935	0.860	0.640	0.414	0.269
153	0.956	0.941	0.850	0.622	0.415	0.256

Transducer distances: T_0, 0 mm; T_1, 2 mm; T_2, 325 mm; T_3, 1125 mm; T_4, 1425 mm; T_5, 1495 mm.

Since R, within the experimental range turns out to be only a function of inlet subcooling, ΔT_{sub}, and not dependent on either inlet pressure or inlet temperature, the correlation obtained has the following form:

$$R = \exp\left[a\left(\frac{Q_a}{Q_{c0}}\right)^{0.5} + b\Delta T_{sub}\right], \qquad [1]$$

with $a = 3.61\ 10^{-3}$ and $b = 1.55$.

The comparison between experimental data and predictions by means of [1] is plotted in figure 4 for the initially subcooled tests. The agreement is quite satisfactory, most of the data lying within a $\pm 10\%$ band from the correlation [1] line (r.m.s. error = 7.26%). Saturated liquid tests are badly predicted, essentially because of the experimental uncertainty already described (see table 1).

The use of [1] requires knowledge of the reference mass flux, G_{c0}, (from which Q_{c0} can be calculated) to obtain the mass flux in the presence of air, G_c. G_{c0} may be obtained either from

Table 3

	Temperatures (°C)					
	T_0	T_1	T_2	T_3	T_4	T_5
20	143.05	143.54	143.30	143.30	143.05	138.38
21	141.08	141.57	140.84	140.10	138.87	133.46
22	141.57	141.82	141.08	140.35	138.62	133.46
24	140.59	140.84	139.61	138.87	136.66	131.25
25	140.35	140.59	139.12	138.13	135.43	129.53
27	140.10	140.10	138.38	137.64	135.18	130.02
28	140.35	140.59	139.61	139.36	137.89	133.46
29	140.35	140.59	139.85	139.12	137.64	132.24
30	139.36	139.36	136.17	135.67	131.01	125.11
31	139.36	139.61	136.90	135.67	131.01	127.57
32	139.61	139.85	137.64	137.15	133.71	128.80
33	139.85	140.10	139.85	140.10	139.61	134.94
34	140.10	140.35	140.10	140.35	139.85	134.69
35	140.10	140.35	140.10	140.35	140.10	133.95
36	139.61	139.85	139.36	139.36	138.62	134.69
37	139.61	139.85	139.61	139.61	139.12	134.20
38	139.85	140.10	139.85	139.85	139.36	135.43
39	140.10	140.35	139.85	139.61	138.62	134.69
40	139.61	139.85	139.36	139.36	138.62	133.71
41	139.85	140.10	139.85	139.61	139.12	135.18
42	139.61	139.85	139.12	139.61	139.12	133.71
43	139.85	140.35	139.85	140.10	139.85	133.22
44	140.10	140.59	140.35	140.59	140.35	133.22
126	147.72	147.72	148.22	147.48	144.03	127.57
127	148.22	147.97	145.76	142.31	132.73	117.75
128	149.94	149.69	148.22	143.54	133.95	119.22
129	149.20	148.71	147.72	142.31	132.97	119.96
130	149.45	147.97	145.26	137.15	129.29	117.51
131	150.68	150.68	150.43	147.23	143.79	127.57
132	150.43	149.94	148.46	140.84	133.46	121.92
133	149.20	148.22	147.72	142.56	137.89	122.41
134	144.28	142.31	141.08	136.66	126.83	111.87
135	149.45	144.03	146.74	143.05	132.73	117.02
136	148.22	147.23	146.25	138.13	133.71	124.87
154	177.79	177.54	178.28	173.10	161.27	143.79
137	177.79	178.04	178.04	172.85	160.28	143.79
138	177.05	176.31	174.33	168.17	152.65	134.69
145	176.80	176.31	173.10	165.70	150.68	131.74
146	176.56	176.31	175.08	168.17	159.54	146.99
147	177.05	176.80	172.61	164.22	150.18	130.76
148	174.33	173.35	174.09	171.62	166.20	151.42
149	174.83	174.33	171.37	166.20	151.42	133.71
150	177.05	174.83	165.70	156.09	143.05	128.80
151	176.56	175.32	172.36	166.20	150.43	129.78
152	175.08	174.58	172.11	167.68	154.86	132.73
153	176.80	175.57	164.22	156.34	143.79	127.08

Transducer distances as for table 2.

available experimental data, or from correlations and models which allow its evaluation. A model proposed by the authors (Celata *et al.* 1985) enables a simple but accurate prediction of G_{c0} and was used to obtain the predictions shown in figure 4.

The theoretical approach

The starting point in this case, which should be called "semi-theoretical", is represented by a simplified design expression for the evaluation of the critical mass flux, proposed previously by the authors (Celata *et al.* 1983a). This expression is based on the assumption that the outlet critical pressure, p_c, is practically equal to the saturation pressure corresponding to the inlet temperature $T_0, p_{sat}(T_0)$:

$$p_c \simeq p_{sat}(T_0).$$

Applying the known expressions for calculation of the pressure drop between the inlet and exit

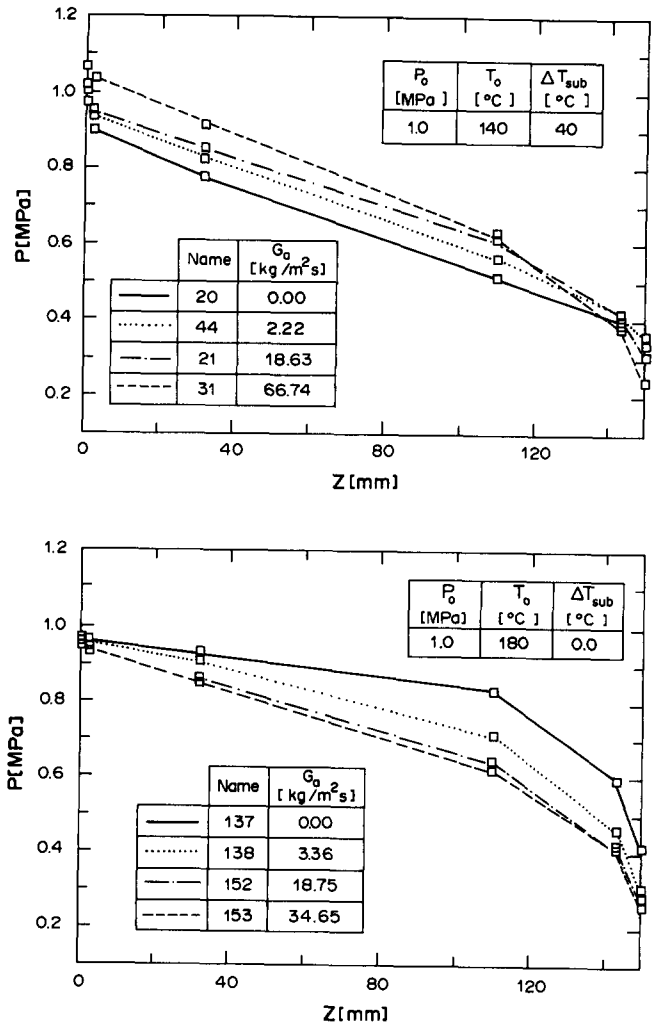

Figure 2. Typical pressure profiles along the test section for subcooled and saturated tests.

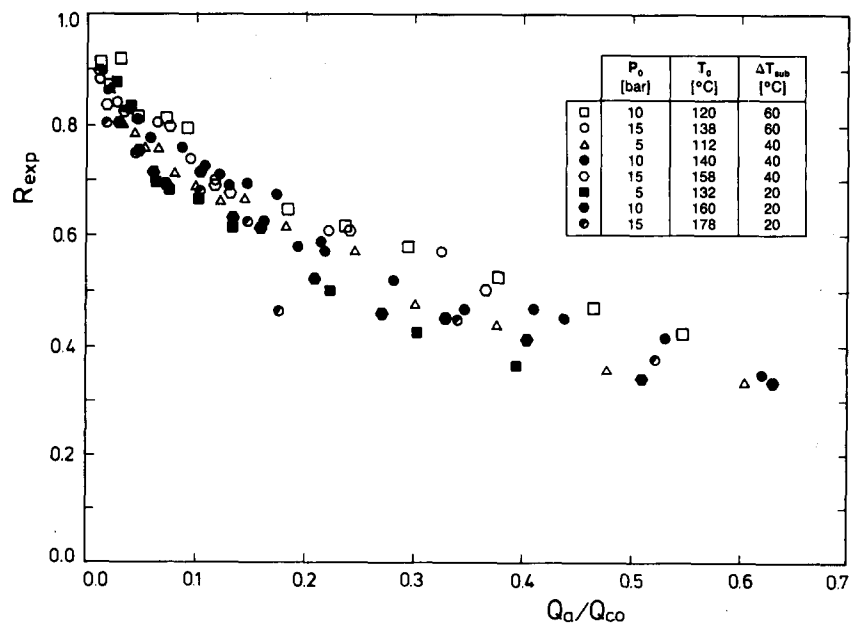

Figure 3. Experimental data of critical mass flow rate in presence of air as a function of the air volumetric flow rate.

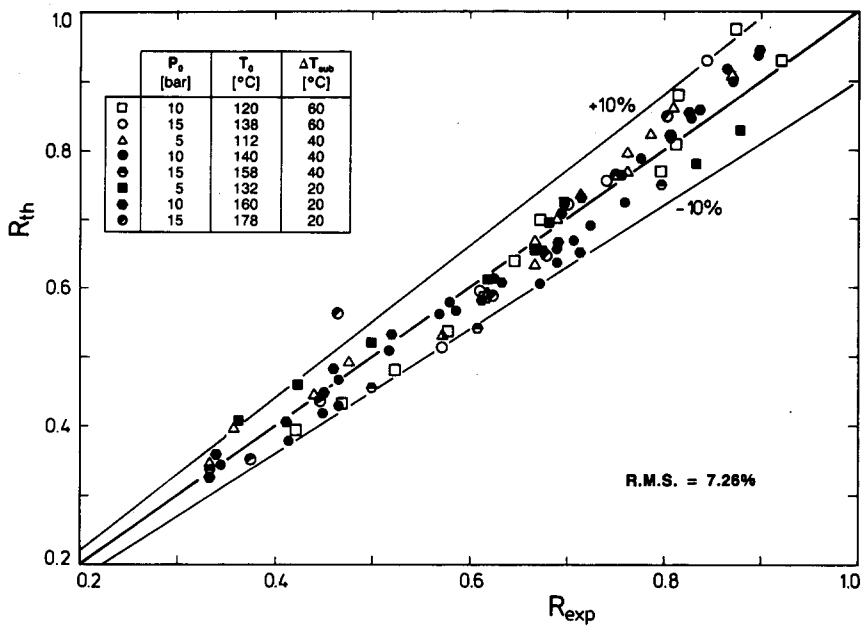

Figure 4. Predictions of R using the empirical correlation [1].

of the channel, one obtains

$$G_c = \sqrt{\frac{2[p_0 - p_{sat}(T_0)]}{v_{f0}\left(K_i + f\frac{L}{D}\right)}}, \qquad [2]$$

with

v_{f0} = specific volume of the liquid at temperature T_0,

K_i = loss coefficient (derived from handbooks or experimentally deduced with cold water tests),

f = friction factor,

L = channel length

and

D = channel diameter.

Equation [2] holds for inlet subcoolings as low as 15–20°C.

Taking into account now the presence of air in the steam–water mixture, the total pressure drop along the discharging channel can be expressed as

$$p_0 - p_{sat}(T_0') = \left[\left(K_i' \bar{v}_0 + f' v' \frac{L}{D}\right) + 2(\bar{v}_1 - \bar{v}_0)\right]\frac{G_c^2}{2}, \qquad [3]$$

where

$(\bar{v}_1 - \bar{v}_0)G_c^2$ = the pressure drop due to the acceleration of the air–water mixture because of the air expansion between $p = p_0$ and $p = p_{sat}(T_0)$,

T_0' = the new stagnation (inlet) temperature after the injection of the cold air in the stagnation region: in the range of the flow rates involved, practically we have $T_0' \simeq T_0$,

K_i' and f' refer to the situation in the presence of air,

$$\bar{v}_0 = (1 - x_a)v_{f0} + x_a v_{a0},$$

$$v_{a0} = v_a(p_0, T_0),$$

$$\bar{v}_l = (1 - x_a)v_{f0} + x_a v_{al},$$

$$v_{al} = v_a[p_{sat}(T_0), T_0],$$

$$\bar{v} = \frac{\bar{v}_0 + \bar{v}_l}{2},$$

$$x_a = \frac{\Gamma_a}{\Gamma} = \frac{G_a}{G_a + G_c} \simeq \frac{G_a}{G_c} = \frac{G_a}{RG_{c0}}$$

and

$$(1 - x_a) = \frac{\Gamma_c}{\Gamma} = \frac{G_c}{G_a + G_c} \simeq 1.$$

Considering an isothermal air expansion between $p = p_0$ and $p = p_{sat}(T_0)$, v_{al} can be obtained from

$$v_{a0} = \frac{ZT_0}{p_0}$$

and

$$v_{al} = \frac{ZT_0}{p_{sat}(T_0)},$$

where

$$Z = 287.1 \text{ J/kg K}.$$

Consequently, we have

$$\bar{v}_0 = v_{f0} + \frac{G_a v_{a0}}{RG_{c0}}$$

$$\bar{v}_l = v_{f0} + \frac{G_a v_{al}}{RG_{c0}}$$

and

$$\bar{v}_l - v_0 = \frac{G_a(v_{al} - v_{a0})}{RG_{c0}}.$$

Solving [3] for G_c, we get

$$G_c^2 = \frac{2[p_0 - p_{sat}(T_0)]}{\left(K_i' \bar{v}_0 + f' \frac{L}{D} \bar{v}\right) + 2(\bar{v}_l - \bar{v}_0)}. \qquad [4]$$

Expressions [2] and [4] neglect the presence and influence of steam in the evaluation of the total pressure drop. On the other hand, this approximation may be allowed because of the reduced steam–water two-phase length in the test channel and the, consequently, small contribution to the total pressure drop; it can be considered realistic for $\Delta T_{sub} > 15$–$20°C$.

According to a procedure typical of the two-phase pressure drop analysis employing two-phase multipliers, it is possible to write

$$K_i' \bar{v}_0 + f' \frac{L}{D} \bar{v} = K_i v_{f0} \phi_l^2 + f \frac{L}{D} v_{f0} \phi_2^2. \qquad [5]$$

It is convenient to use a common air–water two-phase multiplier, ϕ_a^2, so that

$$\left(K_i \phi_l^2 + f \frac{L}{D} \phi_2^2\right) v_{f0} = \left(K_i + f \frac{L}{D}\right) \phi_a^2 v_{f0}, \qquad [6]$$

where K_i and f are the values employed in [2].

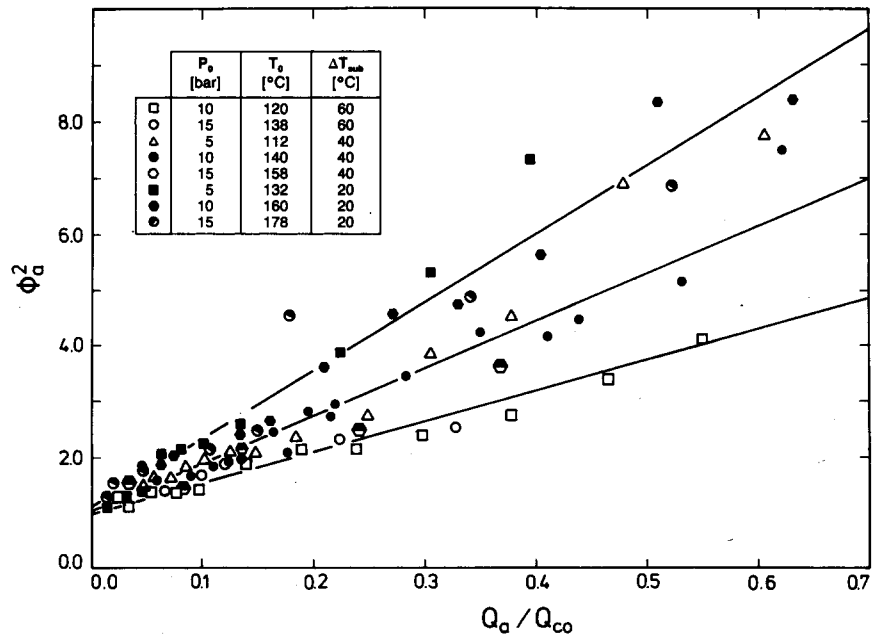

Figure 5. Experimental determination of the air–water two-phase multiplier.

From [2] and [4] it is possible to deduce

$$R^2 = \left(\frac{G_c}{G_{c0}}\right)^2 = \frac{\left(K_i + f\frac{L}{D}\right) v_{f0}}{\left(K_i + f\frac{L}{D}\right) \phi_a^2 v_{f0} + 2(\bar{v}_1 - \bar{v}_0)}. \qquad [7]$$

Substituting into [7] the previously obtained expressions for $\bar{v}_0$ and $\bar{v}_1$ we get

$$R^2 = \frac{v_{f0}}{\phi_a^2 v_{f0} + \dfrac{\dfrac{2}{R}\dfrac{G_a}{G_{c0}}(v_{a1} - v_{a0})}{K_i + f\dfrac{L}{D}}}. \qquad [8]$$

Equation [8] is a second-order equation in R that gives two solutions, only one of which is physically acceptable (the other, being negative, has no physical meaning).

The mathematical solution of [8] and a good prediction of the influence of air on critical flow require knowledge of the air–water two-phase multiplier, which is not generally available from the literature. It is therefore necessary to obtain an expression for ϕ_a^2 from the experimental results.

The experimental results for ϕ_a^2 are reported in figure 5; the expression of the multiplier ϕ_a^2, as a function of Q_a/Q_{c0} and of ΔT_{sub}, has been found to be of the type

$$\phi_a^2 = 1 + C\left(\frac{Q_a}{Q_{c0}}\right)[\exp(-\alpha \Delta T_{sub})]. \qquad [9]$$

From a best-fit procedure through the experimental data we get

$$\alpha = 0.019 \quad \text{and} \quad C = 18.0.$$

The comparison between the values of R obtained from the solution of [8], with the proposed expression of ϕ_a^2, and the experimental values, is reported in figure 6. The agreement is quite satisfactory, even better (r.m.s. error = 5.42%) than that of the empirical approach (r.m.s. error = 7.26%).

Some comments derived by analysing [8] mathematically and comparing the results with what happens in the limit of an idealized situation with no friction ($f = 0$) or geometric losses ($K_i = 0$),

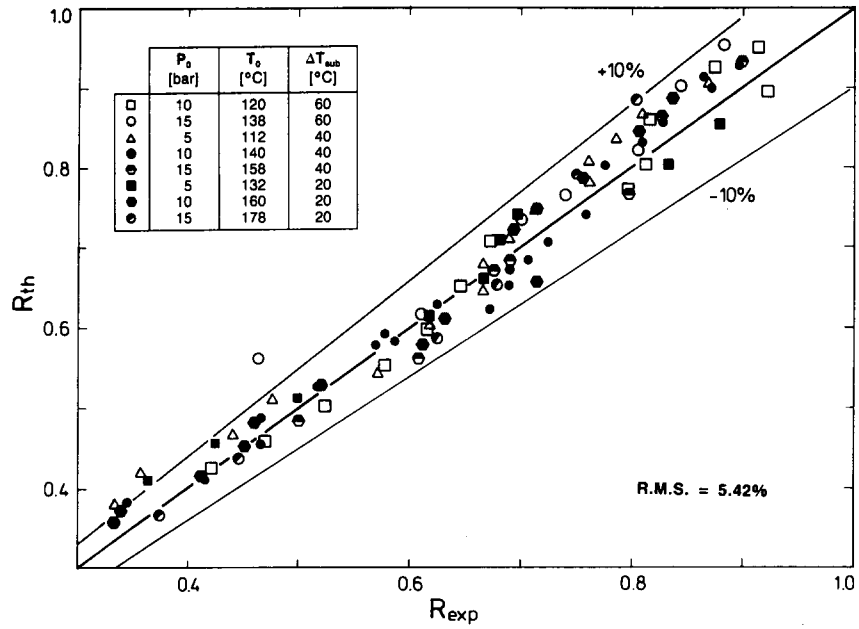

Figure 6. Predictions of R using the theoretical approach, [8].

may be of interest. If only one of the two parameters (f or K_i) is equal to 0 (idealized situation of smooth pipe or no geometric losses) the value of R given by [8] is different from the real situation (both f and K_i different from 0) but not by much. In fact there still exists a resistance to the flow which limits the flow rate, and both G_c and G_{c0} would be affected by a variation of the same order of magnitude. Equation [8] confirms this qualitative consideration. If both f and K_i are set equal to 0, $G_{c0} \to \infty$ (no resistance to the flow); consequently, $R \to 1$ for $G_a \to 0$, and $R = 0$ for $G_a \neq 0$.

In fact in the latter case the pressure drop due to the acceleration of the air–water mixture would represent the resistance to the flow. These limits are both respected by [8], which is easy to verify.

5. CONCLUDING REMARKS

An experiment devoted to the study of the influence of non-condensible gas on steam–water two-phase critical flow is reported.

Using data analysis we have obtained an acceptable theoretical prediction of experimental values in the case of initially subcooled liquid flows, either by means of an empirical approach or by means of traditional considerations and correlations for two-phase and single-phase pressure drop.

Acknowledgements—The authors wish to thank Mr G. Cipolla and Mr O. Levati who performed the experimental runs. Thanks are also due to Mrs B. Perra for her helpful assistance in editing the paper.

REFERENCES

ARDRON, K. H. 1978 A two-fluid model for critical vapour–liquid flow. *Int. J. Multiphase Flow* **4**, 323–337.

CELATA, G. P., CUMO, M., FARELLO, G. E. & INCALCATERRA, P. C. 1983a Critical flows of subcooled liquid and jet forces. Presented at *ASME–AIChE National Heat Transfer Conf., Seattle, Wash.*

CELATA, G. P., CUMO, M., D'ANNIBALE, F. & FARELLO, G. E. 1983b Two-phase boundary layers in critical flows. In *Proc. Colloque Euromech 176, Grenoble.*

CELATA, G. P., CUMO, M., D'ANNIBALE, F. & FARELLO, G. E. 1985 A computation method for mass flow rate predictions in critical flows of initially subcooled liquid in long channels. *Heat Technol.* **3**(3/4), 24–42.

CELATA, G. P., CUMO, M., D'ANNIBALE, F. & FARELLO, G. E. 1986a Critical flows in nuclear reactor safety. In *Proc. 2nd Latin American Congr. on Heat and Mass Transfer*, São Paulo, Brazil.

CELATA, G. P., CUMO, M., D'ANNIBALE, F. & FARELLO, G. E. 1986b Two-phase flow models in unbounded two-phase critical flows. *Nucl. Engng Des.* **97,** 211–222.

DOBRAN, F. 1985 Non-equilibrium modeling of two-phase critical flow in pipes and jet expansion region. Presented at *Specialist Mtg on Small Break LOCA Analyses in LWR's*, Pisa.

FLINTA, J. 1983 Critical flow in reactor safety analysis. Presented at *European Two-phase Flow Group Mtg*, Zurich.

HENRY, R. E. 1968 A study of one and two component, two-phase critical flows at low qualities. ANL Report-7430.

HENRY, R. E. 1970a The two-phase critical discharge of initially saturates or subcooled liquid. *Nucl. Sci. Engng* **41,** 336–342.

HENRY, R. E. 1970b An experimental study of low quality, steam–water critical flow at moderate pressure. ANL Report-7740.

HENRY, R. E. & FAUSKE, H. K. 1971 The two-phase critical flow of one-component mixtures in nozzles orifices and short tubes. *ASME Jl Heat Transfer* **95,** 179–187.

ILIC, V., BANERJEE, S. & BEHLING, S. 1986 A qualified database for the critical flow of water. EPRI Report NP-4556.

LACKMÉ, C. 1982 Thermodynamics of critical two-phase discharge from long pipes of initially subcooled water. In *Heat Transfer in Nuclear Reactor Safety* (Edited by BANKOFF, S. G. & AFGAN, N. H.), pp. 391–407. Hemisphere, Washington, D.C.

MOODY, F. J. 1965 Maximum flow rate of single component two-phase mixture. *ASME Jl Heat Transfer* **86,** 134–142.

MOODY, F. J. 1966 Maximum two-phase vessel blowdown from pipes. *ASME Jl Heat Transfer* **87,** 285–295.

Proc. Wkshp on Jet Impingement and Pipe Whip (Sponsored by ENEA and AMN), Genoa 1981.

Proc. IAEA Specialist Mtg/Wkshp on Experimental and Modeling Aspects of Small Break LOCA, Budapest 1983.

Proc. Specialist Mtg on Small Break LOCA Analyses in LWRs, Pisa 1985.

REOCREUX, M. 1974 Contribution to the study of critical flow rates in two-phase water–vapour flow. Thesis, Univ. of Grenoble, France.

REOCREUX, M. 1976 Experimental study of steam–water chocked flow. In *Proc. CSNI Specialists Mtg, Atomic Energy of Canada*, Vol. 2, pp. 637–669.

WEIGAND, G. G., THOMPSON, S. L. & TOMASKO, D. 1983 Two-phase jet loads. Report NUREG/CR-2913.